# CHARACTERISATION OF SOLAR CELLS AND MODULES UNDER ACTUAL OPERATING CONDITIONS

## W. DURISCH[1], J. URBAN[2] AND G. SMESTAD[3]

[1]Paul Scherrer Institut, PSI, CH-5232 Villigen PSI, Switzerland

[2]Technical College Ulm, FHU, D-89075 Ulm, Germany

[3]Earth Systems Science and Policy, California State
University at Monterey Bay, CSUMB, 100 Campus Center,
Seaside California 93955-8001, California, U.S.A.

## ABSTRACT

A PC-based measuring system is presented for outdoor testing of solar cells and modules under real operating conditions. It consists of a sun-tracked sample holder, different electronic loads (including control), digital multimeters, a PC and a laser printer. Insolation is measured and recorded with pyranometers, pyrheliometers and a reference cell. Current-voltage curves are acquired in the range of irradiance from 10 $W/m^2$ to over 1000 $W/m^2$. Small single cells of size down to 3 mm by 3 mm as well as large modules and laminates up to 1 m by 1.5 m can be tested. The measurement time for one test can be varied between 5 to 15 seconds. The maximum power point (mpp) is normally detected on-line. However, it can also be determined in a subsequent mathematical analysis, if more precise mpp data are required. The maximum relative uncertainty in the efficiency (determined from mpp data) has been estimated to be less than ± 1 %, depending on type and size of cell or module and on the constancy of the insolation during the testing time. Using a new dynamic method, the temperature coefficient of the efficiency can be determined within a relative uncertainty of about ± 3 %. The coefficient is used to derive standard test condition data. Results are given for two commercial modules.

## KEYWORDS

Photovoltaic test stand; solar cell efficiency; temperature coefficient of efficiency; I-V characteristic; cell temperature; irradiance measurement; maximum power point detection; sun-tracker; error estimations.

## INTRODUCTION

Photovoltaic (PV) probably is the most elegant way to convert solar energy into electricity. However, the technology is not yet commercially competitive for high volume generation of electricity. Nevertheless there are more and more applications for which photovoltaic by far is the best solution (Durisch et al., 1987), thus guaranteeing a steadily growing market. According to predictions by many energy experts, photovoltaic electricity will necessarily play a significant role in any sustainable energy future. The future competitiveness of PV depends on many factors, such as technological advances, production volume of PV components, ecological tax on traditional energies, and also on the most judicious use of this new energy technology. The latter point in particular relates to the performance of PV-generators under site specific climatic conditions. The question is: What energy output of different generators can be expected under actual operating conditions at climatologically different sites? To answer this question, the physical

behaviour of solar cells and photovoltaic modules under varying solar illumination and changing ambient temperature needs to be known. Usually these data are not provided by the manufacturers and suppliers of PV products. Moreover, the data provided most often are taken at test conditions which never occur in practice. In the present paper, therefore, data on two selected modules under real operating conditions are provided. For this purpose a flexible test stand for outdoor characterisation of single cells and modules was developed, tested, and successfully put into operation at PSI. The purpose of the data furnished is to support appropriate design and optimum utilization of PV power supply systems, and thus to improve their economic attractiveness. This is achieved by using outdoor data together with site specific, time-resolved meteorological data (e.g. Durisch et al., 1995, 1996) as input for simulation models which are used to calculate the specific daily, monthly and yearly electricity production of different PV generators. The use of outdoor data leads to reliable results and enables the selection of the most suited module type for a specified application at a selected site. Knowing that simulations with Standard Test Condition (STC) data can lead to an overestimation of the production by up to 40% (Bücher and Heidler, 1993), it is important that outdoor test data are used to provide a realistic assessment of the productivity of PV generators.

## TEST STAND/MEASUREMENT METHODS

In Fig. 1 the measurement system is schematically represented. As sun tracker a parallactic mount for telescopes was modified to allow solar cells and modules to follow the sun's orbit. The daily change in the
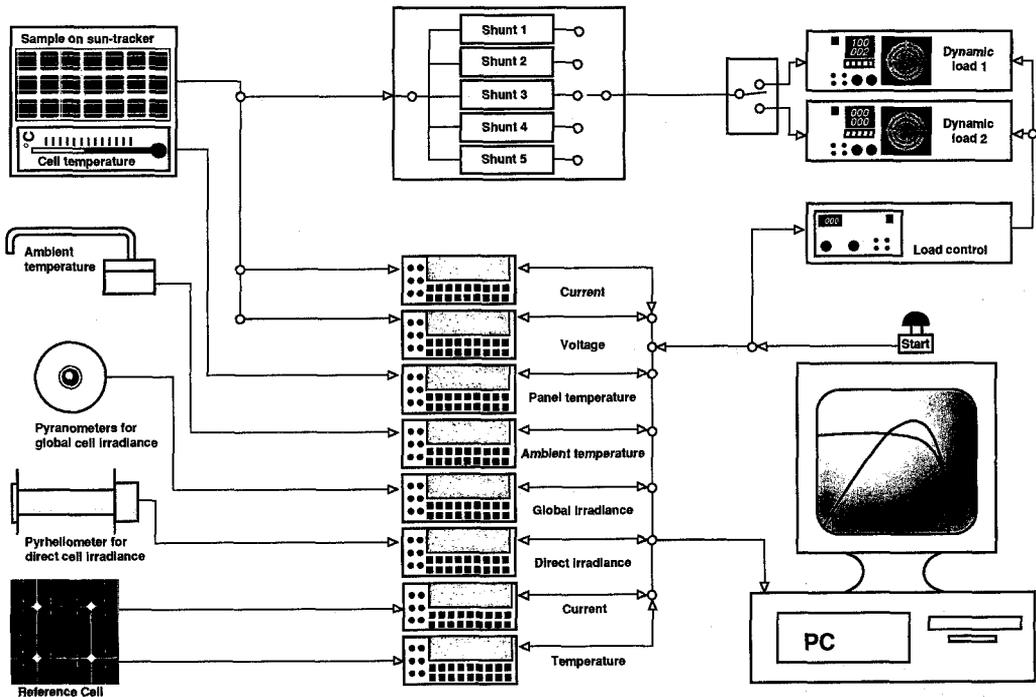


Fig. 1. Schematic representation of the measurement system for the characterisation of solar cells and modules. Sensors for wind speed and direction are not shown in this Figure.

sun's declination is taken into account by a specially developed crank mechanism. Both axes, the polar as well as the declination, are driven by step motors via reduction and worm gears. For both motors a simple open-loop control provides precise tracking of the sun throughout the year. Beside the cells and modules, the tracker also carries six pyranometers (CM 21, Kipp & Zonen, 305 - 2800 nm) and a reference cell (SIEMENS). They are used to measure the insolation incident on the cells and modules. To increase the accuracy of the pyranometrically measured global irradiance $G_n$, (W/m$^2$) in the cell and module plane respectively, the pyranometers are connected in series. The ambient temperature is measured using a ventilated and shielded Pt-100-sensor. The direct normal irradiance $I_n$, is measured with pyrheliometers (Eppley) mounted on extra trackers developed by PSI. $I_n$ is needed to calculate the diffuse irradiance. Wind speed and direction are also measured. All the meteorological signals as well as the voltage signal V, of the sample under test are transmitted to the PV laboratory, where they are measured by digital multimeters (FLUKE 8842A, 5½ digit and PREMA 6001, 6½ digit). The current I, from the sample is measured via high precision resistors (shunts) having very low temperature coefficients. To measure the temperature in the cell, Pt-100 surface sensors (6 mm by 6 mm) are soldered on the rear side of the cells. For the modules the back-sheet is opened, and the sensor is directly attached to the back side of a cell. From the multimeters the
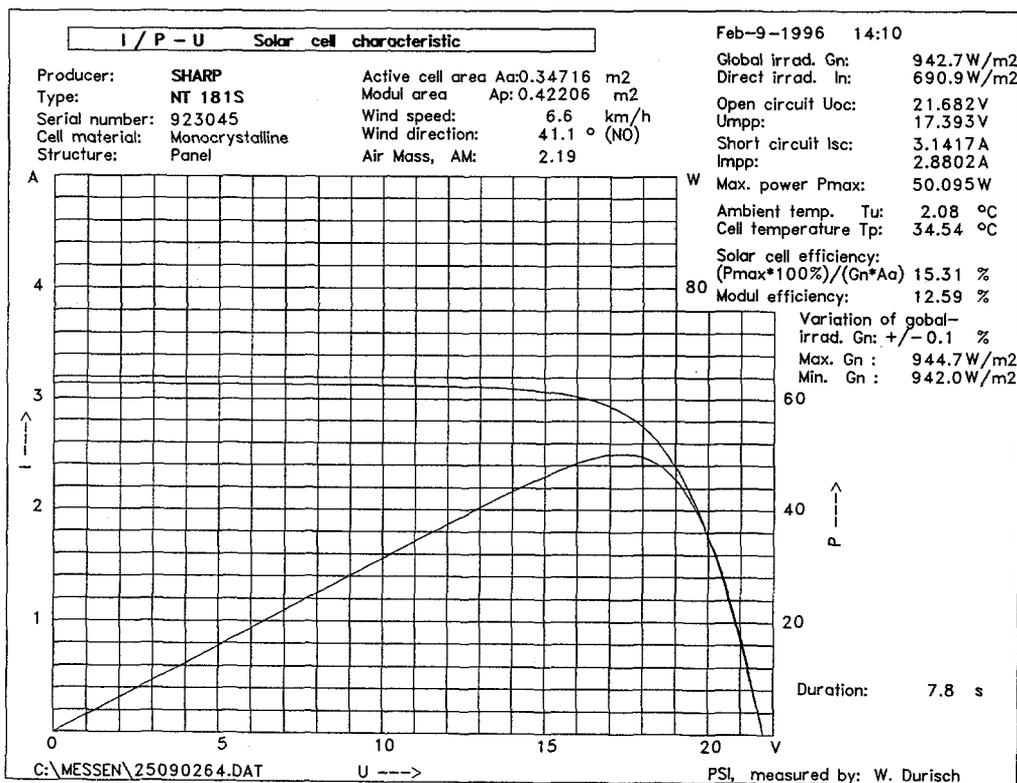


Fig. 2.   Current voltage and power voltage curves and characteristic data of a selected module under actual operating conditions. Before performing the test, the module was run under maximum power point conditions during about 15 minutes, leading to thermal equilibrium. The Air Mass AM, is calculated from the actual sunposition.

signals are sent to a DEC PC 560 XL via IEEE bus. About 120 data points are taken in a period of approximately 7 seconds. They are evaluated on-line, so that the current voltage (I-V) and power voltage (P-V) curves together with all relevant characteristic data appear on the screen. The curves and data on the screen can be printed in identical form on a HP Laser Jet to provide a test record, Fig. 2. To scan the whole voltage range from short to open circuit conditions, different dynamic loads are available, covering a wide range of powers absorbed. The maximum power point (mpp) is detected on-line by searching for the highest power $P_m$, reached during an I-V scan. Knowing the global irradiance $G_n$ in this point, the active cell area $A_a$ and the module (panel) area $A_p$, the cell and module efficiency $\eta_a$ and $\eta_p$ respectively, can be calculated. Since the P-V data pairs are discretely measured points, a fit $P = (a + b \cdot \exp(cV) + eV)V$ in the neighbourhood of $P_m$ can optionally be performed, from which $P_m$ can be found by mathematical methods. Tests have revealed that the difference in the two $P_m$ detection methods is normally less than 0.02 %. The temperature coefficient of the efficiency is determined from a series of efficiency measurements taken at constant insolation and varying cell temperature, e.g. during warming up of the cell or module from ambient to equilibrium temperature, Fig. 3.

Compared to indoor tests, the most important advantages of outdoor testing are:

a) no expensive artificial light source is required,

b) no limitation in the size of the samples,

c) homogeneous illumination of the samples,

d) testing is possible under varying fraction of diffuse to global irradiance (10 to 100 %),

e) effect of snow- and sand-reflected light can be investigated (Durisch et al., 1989).

The disadvantages of outdoor testing are:

a) available testing time at high insolation levels is limited, demanding flexible experimental scheduling. This handicap is less pronounced in sunny countries. Furthermore, this disadvantage is relaxed by the short acquisition time of 5 to 15 seconds per I-V curve, permitting up to 100 runs per hour.

b) transformation of measurement results to Standard Test Conditions, STC (25 °C, 1000 W/m$^2$ and AM 1,5) is required, if comparison with such data is desired.

## RESULTS

In Figs. 3 and 4 the results are presented for two commercially available modules. Both consist of monocrystaline silicon cells encapsulated between glass and tedlar. The modules are specified by the manufactures to produce, under STC conditions, maximum powers of 55 W and 85 W, respectively. With each module about 100 I-V runs were performed. In Fig. 3 the efficiencies of the two modules are shown at constant irradiance $G_n$, and varying cell temperature $\vartheta$. These data were used to determine the temperature coefficients of the efficiency of the two modules, table 1 (see also eq. (6) in following paragraph). Using these coefficients and additional $\vartheta_i/\eta_i$-measurements, the corresponding efficiencies $\eta_{25}$ at 25 °C for varying irradiance were determined according to eq. (10) in the next paragraph. The result is presented in Fig. 4. Good fits of the data points of Fig. 4 were achieved as follows:

$$Module\ 1 \quad \eta_{25} = p_1 G_n + p_2 \sqrt{G_n} + p_3 \sqrt[3]{G_n} + p_4 \sqrt[4]{G_n} + p_5 \sqrt[5]{G_n} \tag{1}$$

$$Module\ 2 \quad \eta_{25} = q_1 G_n + q_2 G_n / (q_3 + G_n) \tag{2}$$

Knowing the parameters $p_i$ and $q_i$, these equations can be used to calculate the yearly electricity production of the modules 1 and 2.

The parameters $p_i$ and $q_i$ were found to be:

$p_1 = -0.02864$  $p_2 = 13.4543$  $p_3 = -168.184$  $p_4 = 408.257$  $p_5 = -249.937$

$q_1 = -0.00487$  $q_2 = 23.01$  $q_3 = 188.1$

Table 1. Efficiencies $\eta_z$ and $\eta_{25}$ at 0 °C and 25 °C, and temperature coefficient b of the efficiency $\eta$ of two selected modules. Also given are their relative uncertainties.

| Test-sample | $\eta_z$ % | $\eta_{25}$ % | b %/°C | $\Delta\eta_z/\eta_z$ % | $\Delta\eta_{25}/\eta_{25}$ % | $\Delta b/b$ % |
|---|---|---|---|---|---|---|
| Module 1 | 17.37 | 15.65 | -0.0685 | 0.33 | 0.45 | 2.4 |
| Module 2 | 15.97 | 14.72 | -0.0500 | 0.38 | 0.48 | 2.9 |

Note: The figures in this table for module 1 result from measurements at $G_n = (1008 + 45/- 18)$ W/m$^2$ and AM = 1.57 ± 0.02. For module 2 the measurements were performed at $G_n = (860 ± 25)$ W/m$^2$ and AM = 2.35 ± 0.06. The table also contains results dealt with in the following chapter

The fitted curves in Fig. 4 exhibit maximum efficiencies of 16.05 % at $G_n = 661$ W/m$^2$ for module 1 and of 14.74 % at $G_n = 754$ W/m$^2$ for module 2. At $G_n = 1000$ W/m$^2$, the fits in Fig. 4 yield 15.76 % and 14.50 % for the two modules. These are slightly different from the corresponding values found from the $\eta/\vartheta$-fits in Fig. 3 at 25 °C, listed as $\eta_{25}$ in table 1. One reason is that the $\eta/\vartheta$-fit and the $\eta_{25}/G_n$-fit were performed independently from each other. An other reason might be, that with module 2 the $\eta/\vartheta$-measurements were not performed at $G_n \approx 1000$ W/m$^2$ but at $G_n \approx 860$ W/m$^2$. Nevertheless, the small differences between the independently determined values confirm the reliability of the measured date. The manufacturer gives the STC efficiencies as 16 % for module 1 and 16.3 % for module 2. While for module 1 the agreement with our results is within the uncertainty estimated in the following chapter, module 2 deviates by about minus 10 %. (Note: All efficiencies given above refer to the active cell area as measured by the present authors). Furthermore, at low intensities module 2 shows significant lower efficiencies than module 1.
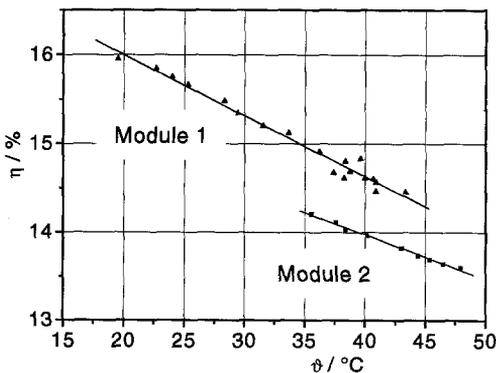
Fig. 3  Efficiencies of two commercially available modules at constant irradiance as a function of the cell temperature $\vartheta$. See also Table 1.
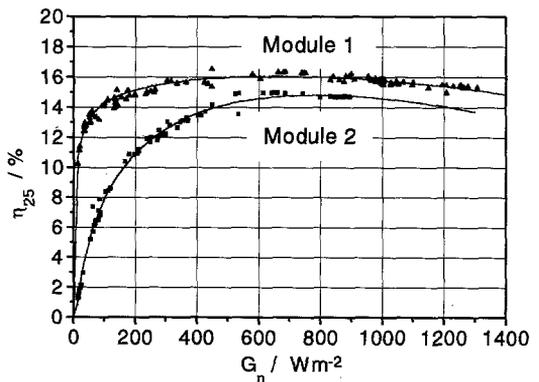
Fig. 4  Efficiencies $\eta_{25}$ at 25 °C of modules 1 and 2 of Fig. 3 as a function of the global normal irradiance $G_n$ incident on the modules.

# ERROR CONSIDERATIONS

The efficiency is one of the key parameters in power generation, including photovoltaics. The determination of the efficiency, however, is usually difficult and subject to many sources of errors. Therefore thorough error analyses have been performed with respect to the efficiency and its temperature coefficient.

For the efficiency of a solar cell or module, operated in the maximum power point mpp, the relation

$$\eta = IV / (AG) \qquad (3)$$

holds. For the sake of simplicity, subscripts referring to the maximum power point mpp and to the active cell area $A_a$ and panel area $A_p$ as well as referring to the global normal irradiance $G_n$ are omitted.
From the law of propagation of errors one gets:

$$\Delta\eta / \eta = \sqrt{(\Delta I / I)^2 + (\Delta V / V)^2 + (\Delta A / A)^2 + (\Delta G / G)^2} \qquad (4)$$

While the terms $\Delta I/I$, $\Delta V/V$ and $\Delta A/A$ can easily be estimated from the specifications of the measuring instruments and precision resistor used, the term $\Delta G/G$ needs special attention, since G is obtained, as mentioned, by a series connection of six pyranometers, producing a voltage $V_G$. The sensitivities $s_i$ of the pyranometers and their standard deviations $\Delta s_i$ are known from calibrations at the World Radiation Centre WRC at Davos, Switzerland. Using this information, the following relation is obtained for $\Delta G/G$:

$$\Delta G / G = \sqrt{(\Delta V_G / V_G)^2 + (\Sigma(\Delta s_i)^2) / (\Sigma s_i)^2} \qquad (5)$$

For the test represented in Fig. 2 the following numerical values were obtained:

| | | | | | |
|---|---|---|---|---|---|
| $\Delta V_G/V_G$ | = | 0.022 % | $\Delta A/A$ | = | 0.42 % |
| $\Sigma s_i$ | = | 70.49 mV/(kWm$^{-2}$) | $\Delta V/V$ | = | 0.035 % |
| $\Sigma (\Delta s_i)^2$ | = | 0.021 (mV/(kWm$^{-2}$))$^2$ | $\Delta I/I$ | = | 0.036 % |

From these values one obtains: $\Delta G/G = 0.21$ % and $\Delta\eta/\eta = 0.47$ %. We note that systematic errors are not included in the analysis performed so far. Taking them into account a relative uncertainty of about $\pm$ 1 % in the efficiency is conservatively estimated. For the test presented in Fig. 2 this means: $\eta = (15.31 \pm 0.15)$ % or 15.2 % $\leq \eta \leq$ 15.5 %. With the assumption that systematic errors can be neglected, the efficiency is in the range 15.24 % $\leq \eta \leq$ 15.38 %. From the above analysis it is concluded that the determination of the cell and module area deserves special attention. Furthermore, from eq. (5) it follows that by the series connection of six pyranometers the uncertainty $\Delta G/G$ is reduced approximately by a factor of $1/\sqrt{6}$ from, typically, 0.5 % down to 0.2 %, as compared to the measurement of G with one single pyranometer. Regarding the uncertainty $\Delta A/A$ it should be mentioned that for single nonencapsulated cells this value is lower than for modules, since more precise measuring methods can be applied.

The efficiency of a cell or module being operated at the maximum power point depends on the cell temperature $\vartheta$ , the irradiance Gn, the spectral composition of the incident sunlight and possibly also on other parameters. If all parameters except the cell temperature are constant, the efficiency is found to be a linear function of the cell temperature $\vartheta$

$$\eta = \eta_z + b\vartheta \qquad (6)$$

As shown in Fig. 3, this simple relation holds at least in the range of interest, i.e. from 20 °C to 50 °C and for the modules tested. From a set of n measured points ($\vartheta_i$, $\eta_i$) the parameters $\eta_z$ and b are found by a least

squares fit, b being the temperature coefficient of the efficiency $\eta$. Assuming that the measured values of $\vartheta_i$ are much more accurate than those for $\eta_i$, the mean relative errors of b and $\eta_z$ are

$$\Delta b / b = \sqrt{n\Sigma(\eta_z / b + \vartheta_i - \eta_i / b)^2 / \left[(n-2)(n\Sigma\vartheta_i^2 - (\Sigma\vartheta_i)^2)\right]} \tag{7}$$

$$\Delta\eta_z / \eta_z = (\Delta b / b)(b / \eta_z)\sqrt{\Sigma\vartheta_i^2 / n} \tag{8}$$

For the STC temperature $\vartheta_0 = 25$ °C one now gets

$$\Delta\eta_{25} / \eta_{25} = \sqrt{\left[\eta_z^2(\Delta\eta_z / \eta_z)^2 + b^2\vartheta_0^2(\Delta b / b)^2\right] / (\eta_z + b\vartheta_0)^2} \tag{9}$$

The measurement of the cell temperature $\vartheta$ is performed with calibrated Pt-100 sensors applying the four-wire technique and a high precision digital multimeter, thus guaranteeing an accuracy within in few hundredths of a degree. Therefore the above-mentioned assumption on the higher accuracy of the temperature measurement compared to the efficiency determination is justified.

## DISCUSSION/CONCLUSIONS

Strictly speaking the temperature coefficient b and the efficiency $\eta_z$ in eq. (6) are functions of the irradiance $G_n$ and the spectral composition of the light falling on the cells. However, solar cells of crystalline silicon, as investigated in the present paper, are fairly insensitive to spectral changes. If this were not the case, they would not be suitable as sensors for $G_n$-measurements in reference cells. On the other hand, if the measurements ($\vartheta_i$, $\eta_i$) are taken at an irradiance of $G_n \approx 1000$ W/m² and an Air Mass AM $\approx 1.5$, eq. (6) permits an accurate determination of the cell efficiency at STC. AM $\approx 1.5$ occurs under clear sky two times a day at PSI, except from September 25 to March 19, when the sun elevation is permanently below 42 °. Furthermore, if the temperature coefficient b were also insensitive to changes of the irradiance $G_n$, than eq. (6) would also provide an efficient way to study the dependence of the efficiency $\eta$ on the irradiance $G_n$, since then the relation

$$\eta_{25} = \eta(G_n, \vartheta) - b(\vartheta - \vartheta_o) \tag{10}$$

where $\eta(G_n, \vartheta)$ is the efficiency measured at $G_n$ and $\vartheta$ would be valid. The latter assumption either needs bo be verified or a relation $b = b(G_n)$ for crystalline silicon at AM = 1.5 has to be found. Equation (10) was applied to plot the efficiency curves in Fig. 4, based on the assumption that $b \neq b(G_n)$.

The curves of efficiency $\eta_{25}$ vs. irradiance $G_n$ at constant cell temperature, Fig. 4, show maxima at irradiances lower than the STC irradiance of 1000 W/m². A qualitatively similar trend was found with concentrator cells (Bücher and Heidler, 1993). Further investigations with other modules and advanced physical modelling of cells and modules might help to understand this behaviour. A maximum efficiency at irradiances lower than 1000 W/m² is of interest for sites having generally low intensities available. For such sites, module 2 as depicted in Fig. 4 would not be the best choice.

The scattering of the measured points in Fig. 4 is larger than expected from the error analysis. Having in mind that the silicon cell modules inspected are fairly insensitive to spectral changes of the incident solar light, a fourth parameter influencing the efficiency seems to play a role. In this respect it has to be mentioned that the measurements presented in Fig. 4 were performed at different diffuse fractions ($G_n - I_n$)/$G_n$ of the impinging light, ranging from 10 to 100 %. Due to the different thermodynamic qualities of diffuse and direct (beam) irradiance, such an effect can not be excluded and needs further investigation.

From the present work it is concluded that I-V characteristics of solar cells and modules measured under actual operating conditions, combined with site-specific time-resolved meteorological data, provide the best basis for reliable predictions of the electricity production of PV-systems. A similar conclusion was obtained by Ertürk et al. (1996). Production data, however, are indispensable for the assessment of the specific generation cost, being an important factor in future decisions on energy supply options.

## ACKNOWLEDGEMENT

## REFERENCES

Bücher, K. and Heidler, K. (1993). Physikalisches Verhalten und energetische Bewertung von Solarzellen mit einem oder mehreren Übergängen unter realistischen Bezugsbedingungen. BMFT Status-Seminar Photovoltaik.

Durisch, W., Bühlmann, M., Kesselring, P. and Morisod, R. (1987). Measurements and Operational Experience with a Photovoltaic Plant in the Swiss Alps. ISES Solar World Congress, Hamburg, Proceedings 1, 289-297. Pergamon Press.

Durisch, W., Brack, M., Bulgheroni, W. and Gähwiler, E. (1989). Albedo Measurements and System Performance of a Grid-Connected Photovoltaic Plant in the Swiss Alps. ISES Solar World Congress, Kobe, Japan, Proceedings 1, 336-340. Pergamon Press

Durisch, W., Keller, J., Bulgheroni, W., Keller, L. and Fricker, H. (1995). Solar Irradiation Measurements in Jordan and Comparison with Californian and Alpine Data. Applied Energy 52, 111-124.

Durisch, W. and Hofer, B. (1996). Klimatologische Untersuchungen für Solarkraftwerke in den Alpen, am Beispiel Laj Alv, Disentis, Graubünden. PSI-Bericht Nr. 96-01, ISSN 1019-0643.

Ertürk, N., Klonk, M. and Machicao y Priemer, M. (1996). Simulation von Solargeneratoren. Technische Universität Berlin, Institut für Elektrische Maschinen. Submitted to SONNENENERGIE.